Synthesis of Zirconium Complexes Containing the Tridentate Diamido Ligands $[(t\text{-Bu-}d_6\text{-N-}o\text{-}C_6H_4)_2S]^{2-}$ and $[(i\text{-PrN-}o\text{-}C_6H_4)_2S]^{2-}$

David D. Graf, Richard R. Schrock,* William M. Davis, and Rüdiger Stumpf

Department of Chemistry 6-331, Massachusetts Institute of Technology, 77 Massachusetts Avenue, Cambridge, Massachusetts 02139

Received November 17, 1998

The thioethers $(t\text{-Bu-}d_6\text{-NH-}o\text{-}C_6H_4)_2S$ (H_2[t-BuNSN]) and $(i\text{-PrNH-}o\text{-}C_6H_4)_2S$ (H_2[i-PrNSN]) have been prepared in three steps in good yield. Zirconium complexes that contain the $[t\text{-BuNSN}]^{2-}$ ligand ([t-BuNSN]$Zr(NMe_2)_2$, [t-BuNSN]$ZrCl_2$, and [t-BuNSN]$ZrMe_2$) were prepared readily, but the last is unstable, and no higher alkyl homologues could be prepared. In contrast, [i-PrNSN]$ZrMe_2$ and [i-PrNSN]$Zr(CH_2CHMe_2)_2$ are both stable, even at elevated temperatures. An X-ray study of [t-BuNSN]$ZrCl(NMe_2)$ showed it to have a geometry about zirconium that is approximately trigonal bipyramidal with the chloride and sulfur atoms in the axial positions. An X-ray study of [i-PrNSN]$ZrMe_2$ showed it to have approximately a square-pyramidal structure with a methyl group in the apical position. Low-temperature solution ^1H and ^{13}C NMR spectra of $[t\text{-BuNSN}]^{2-}$ and $[i\text{-PrNSN}]^{2-}$ species are consistent with the solid-state structures, although inversion at sulfur on the NMR time scale results in equilibration of the two metal substituents (e.g., methyl groups). Cationic complexes prepared from [RNSN]$ZrMe_2$ precursors (R = t-Bu, i-Pr) were neither stable at 22 °C nor active for the controlled polymerization of 1-hexene.

Introduction

We recently reported that [t-BuNON]$ZrMe_2$, where $[t\text{-BuNON}]^{2-}$ is the tridentate diamido ligand $[(t\text{-Bu-}d_6\text{-N-}o\text{-}C_6H_4)_2O]^{2-}$, upon activation with $[PhNMe_2H][B(C_6F_5)_4]$ or $[Ph_3C][B(C_6F_5)_4]$ in chlorobenzene, will initiate the living polymerization of up to ~500 equiv of 1-hexene.[1] Through ^{13}C labeling studies we showed that living poly(1-nonene) is formed in a 1,2-insertion process, that it is stable and observable by NMR at 22 °C in the absence of excess 1-nonene, and that it decomposes within minutes at 40 °C.[2] The fact that the living polymer is stable in the absence of excess 1-hexene at 22 °C distinguishes this zirconium system from the first reported system for the living polymerization of 1-hexene, one based on titanium complexes that contain a diamido ligand of the type $[ArylNCH_2CH_2CH_2NAryl]^{2-}$ (Aryl = 2,6-i-$Pr_2C_6H_3$, 2,6-$Me_2C_6H_3$),[3−5] since in the titanium system a termination step destroys the catalyst when 1-hexene is depleted.[6] There is no report of $[ArylNCH_2CH_2CH_2NAryl]^{2-}$ zirconium or hafnium complexes behaving in a living manner as initiators for the polymerization of 1-hexene, nor is activated [t-BuNON]$TiMe_2$ a well-behaved initiator for the polymerization of 1-hexene.

We are interested in exploring the utility and versatility of diamido/donor ligands that are related to $[t\text{-BuNON}]^{2-}$. For example, we have recently published syntheses of titanium, zirconium, and hafnium complexes of the type $[(ArylNCH_2CH_2)_2O]MR_2$ (Aryl = a 2,6-disubstituted aryl ring) and the reactivity of activated versions for the polymerization of 1-hexene.[7] We also briefly explored the synthesis and activation of $[(ArylNCH_2CH_2)_2S]ZrMe_2$ for the polymerization of 1-hexene. Activated $[(ArylNCH_2CH_2)_2S]ZrMe_2$ complexes appeared to be relatively well-behaved initiators for the polymerization of 1-hexene, although less stable than initiators derived from the analogous $[(ArylNCH_2CH_2)_2O]ZrMe_2$ compounds. Therefore, we sought also to prepare $[(t\text{-Bu-}d_6\text{-NH-}o\text{-}C_6H_4)_2S]$ (H_2[t-BuNSN]) and zirconium alkyl complexes containing the $[t\text{-BuNSN}]^{2-}$ ligand. We report the results of this effort here. We also explore briefly the role of sterics in the amido alkyl group by preparing $[(i\text{-PrNH-}o\text{-}C_6H_4)_2S]$ (H_2[i-PrNSN]) and complexes that contain the $[(i\text{-PrN-}o\text{-}C_6H_4)_2S]^{2-}$ ligand, and attempting to prepare well-behaved initiators that contain either a $[t\text{-BuNSN}]^{2-}$ or a $[i\text{-PrNSN}]^{2-}$ ligand.

Results

Synthesis of Ligands. H_2[t-BuNSN] was synthesized in four steps that are entirely analogous to those employed to prepare H_2[t-BuNON] (Scheme 1).[1] The

(1) Baumann, R.; Davis, W. M.; Schrock, R. R. *J. Am. Chem. Soc.* **1997**, *119*, 3830.
(2) Baumann, R.; Schrock, R. R. *J. Organomet. Chem.* **1998**, *557*, 69.
(3) Scollard, J. D.; McConville, D. H. *J. Am. Chem. Soc.* **1996**, *118*, 10008.
(4) Scollard, J. D.; McConville, D. H.; Vittal, J. J. *Organometallics* **1995**, *14*, 5478.
(5) Scollard, J. D.; McConville, D. H.; Payne, N. C.; Vittal, J. J. *Macromolecules* **1996**, *29*, 5241.
(6) Scollard, J. D.; McConville, D. H.; Rettig, S. J. *Organometallics* **1997**, *16*, 1810.
(7) Aizenberg, M.; Turculet, L.; Davis, W. M.; Schattenmann, F.; Schrock, R. R. *Organometallics* **1998**, *17*, 4795.

10.1021/om980934k CCC: $18.00
Publication on Web 02/09/1999

Scheme 1

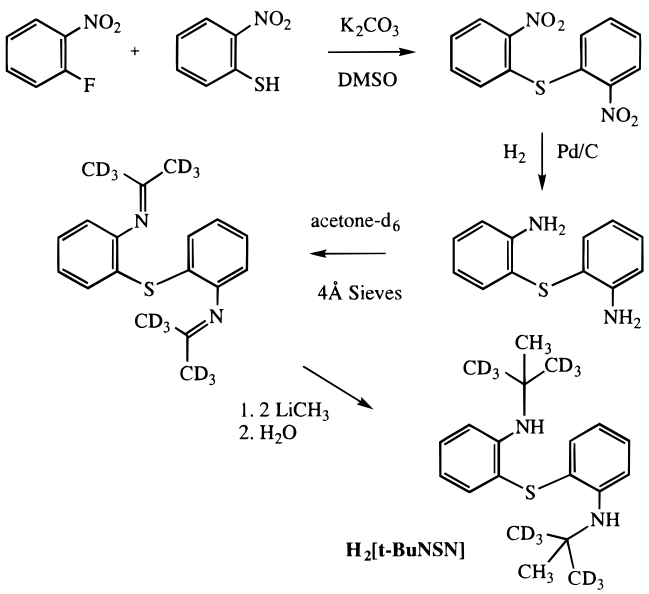

coupling between *o*-$C_6H_4(NO_2)(SH)$ and *o*-$C_6H_4(NO_2)F$ to give $S(o\text{-}C_6H_4NO_2)_2$ and the reduction of $S(o\text{-}C_6H_4NO_2)_2$ to $S(o\text{-}C_6H_4NH_2)_2$ both proceeded in high yield. The reaction between $S(o\text{-}C_6H_4NH_2)_2$ and neat acetone-d_6 (10 equiv) in the presence of activated 4 Å molecular sieves quantitatively provided $S[o\text{-}C_6H_4N{=}C(CD_3)_2]_2$ in 6−10 days. Addition of the diimine to LiMe followed by hydrolysis gave H_2[t-BuNSN] as a light orange solid in ∼50% yield (Scheme 1). As is the case in the synthesis of H_2[t-BuNON], the *tert*-butyl resonance typically integrates as ∼7 protons and is broadened on the right side at the base as a consequence of ∼1 NH proton being exchanged into the CD_3 groups to yield some CD_2H groups at some point during the synthesis of the ligand. NMR spectra suggest that under the reaction conditions at least some H/D exchange occurs before the imine is formed, presumably in acetone-d_6 itself.

H_2[i-PrNSN] was prepared readily in high yield (92%) by the reaction between $S(o\text{-}C_6H_4NH_2)_2$ and acetone in the presence of zinc dust in glacial acetic acid (eq 1). This procedure is based on that reported for the synthesis of a variety of alkylated anilines.[8] H_2[i-PrNSN] was obtained as an oil that sometimes crystallizes after several weeks at room temperature.

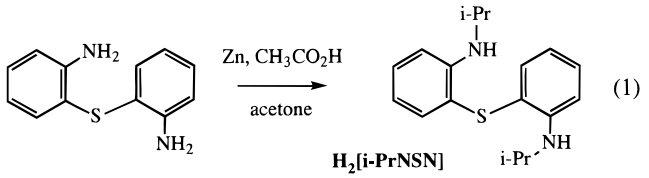

(1)

Syntheses of Zirconium Complexes that Contain [t-BuNSN]$^{2-}$ or [i-PrNSN]$^{2-}$. The reaction between H_2[t-BuNSN] and $Zr(NMe_2)_4$ proceeds cleanly to give [t-BuNSN]$Zr(NMe_2)_2$ as colorless crystals (eq 2). At room

$$H_2[RNSN] + Zr(NMe_2)_4 \xrightarrow{-2Me_2NH} [RNSN]Zr(NMe_2)_2 \xrightarrow{2TMSCl} [RNSN]ZrCl_2 \quad (2)$$
$$R = \text{t-Bu, i-Pr}$$

temperature the reaction is slow (<50% conversion in 48 h), although when the temperature is raised to 60 °C it is complete in 18 h as long as the liberated dimethylamine is periodically removed in vacuo. Recrystallization of the crude product gives colorless blocks of analytically pure [t-BuNSN]$Zr(NMe_2)_2$ in 77% yield. The reaction between H_2[i-PrNSN] and $Zr(NMe_2)_4$ is complete within 4 h at room temperature to give [i-PrNSN]$Zr(NMe_2)_2$ as a yellow oil which occasionally solidifies in cold pentane. The faster reaction between H_2[i-PrNSN] and $Zr(NMe_2)_4$ can be ascribed to the greater ability of the isopropyl-substituted amine to coordinate to Zr in a crowded environment and activate the amine proton toward abstraction by a dimethylamido group.

[t-BuNSN]$Zr(NMe_2)_2$ reacts with 1 equiv of Me_3SiCl in diethyl ether to give [t-BuNSN]$ZrCl(NMe_2)$ (70%) and with excess (4−5 equiv) Me_3SiCl to yield [t-BuNSN]-$ZrCl_2$ (94%; eq 2). [t-BuNSN]$ZrCl_2$ precipitates as a bright yellow solid (>95% pure by NMR) that can be used directly for further reactions. [i-PrNSN]$Zr(NMe_2)_2$ also reacts with an excess (4−5 equiv) of Me_3SiCl in toluene to give [i-PrNSN]$ZrCl_2$ in high yield. By analogy with the observed dimeric structure of [t-BuNON]$ZrCl_2$[9] and because of the relatively low solubility of the [RNSN]$ZrCl_2$ complexes, we propose that [t-BuNSN]-$ZrCl_2$ and [i-PrNSN]$ZrCl_2$ are also dimeric species containing two bridging chlorides.

Thermally unstable [t-BuNSN]$ZrMe_2$ is formed cleanly at −30 °C upon addition of a THF solution of MeMgCl or MeMgI to a diethyl ether solution of [t-BuNSN]$ZrCl_2$. If diethyl ether is employed as the solvent for the Grignard reagent, the resulting [t-BuNSN]$ZrMe_2$ is only ∼80% pure. In diethyl ether or in a diethyl ether/THF mixture LiMe reacts with [t-BuNSN]$ZrCl_2$ to yield decomposition products. [t-BuNSN]$ZrMe_2$ is stable in solution at −30 °C for hours, but it begins to decompose after 30−40 min at 0 °C. Samples are stable in the solid state at −30 °C, but after about 1 h at room temperature some decomposition is observed. Because of the thermal instability of [t-BuNSN]$ZrMe_2$ and our inability to separate it entirely from decomposition products, the glassware employed during workup had to be precooled to −30 °C in order to obtain pure samples. Attempts to make other alkyl complexes (ethyl, isobutyl, neopentyl, and benzyl) from [t-BuNSN]$ZrCl_2$ and Grignard and/or lithium reagents in diethyl ether, THF, or diethyl ether/THF mixtures did not produce any identifiable species that were stable for more than ∼0.5 h at −30 °C. However, we cannot confirm that [t-BuNSN]ZrR_2 species actually were prepared before decomposition ensued; decomposition in the process of preparing the dialkyl species is also a possibility.

[i-PrNSN]$ZrMe_2$ can be synthesized cleanly by treating [i-PrNSN]$ZrCl_2$ with MeMgCl or MeMgI in diethyl ether. In contrast to [t-BuNSN]$ZrMe_2$, [i-PrNSN]$ZrMe_2$ is stable in hydrocarbon solution at room temperature for many (>10) hours and solutions even can be heated to 90 °C for 10 min without any observable decomposition (according to ^{1}H NMR). Surprisingly, the synthesis of [i-PrNSN]$Zr(CH_2CHMe_2)_2$ was also straightforward.

(8) Micovic, I. V.; Ivanovic, M. D.; Piatak, D. M.; Bojic, V. D. *Synthesis* **1991**, *11*, 1043.
(9) Baumann, R. Ph.D. Thesis, Massachusetts Institute of Technology, 1998.

Table 1. Crystal Data and Structure Refinement Details for [t-BuNSN]ZrCl(NMe_2) and [i-PrNSN]$ZrMe_2$[a]

	[t-BuNSN]ZrCl(NMe_2)	[i-PrNSN]$ZrMe_2$
empirical formula	$C_{22}H_{32}ClN_3SZr$[b]	$C_{20}H_{28}N_2SZr$
fw	497.24	419.72
temp (K)	183(2)	173(2)
crystal syst	triclinic	orthorhombic
space group	$P\bar{1}$	$Pna2_1$
a (Å)	9.2816(5)	15.4215(2)
b (Å)	9.8157(6)	15.4052(3)
c (Å)	14.0988(8)	8.3754(2)
α (deg)	85.7090(10)	90
β (deg)	79.3330(10)	90
γ (deg)	68.5410(10)	90
V (Å^3), Z	1174.74(12), 2	1989.75(7), 4
calcd density (Mg/m^3)	1.406	1.401
abs coeff (mm^{-1})	0.683	0.661
F_{000}	516	872
cryst size (mm)	0.18 × 0.18 × 0.12	0.28 × 0.28 × 0.28
θ range for data collecn (deg)	1.47−23.25	1.87−23.26
limiting indices	$-7 \le h \le 10$, $-10 \le k \le 10$, $-11 \le l \le 15$	$-17 \le h \le 17$, $-9 \le k \le 17$, $-8 \le l \le 9$
no. of reflns collected	4906	7711
no. of indep rflns	3320 (R_{int} = 0.0356)	2816 (R_{int} = 0.0286)
no. of data/restraints/ params	3319/0/254	2816/1/218
goodness of fit on F	1.206	0.945
final R indices ($I > 2\sigma(I)$)	R1 = 0.0372, wR2 = 0.0988	R1 = 0.0205, wR2 = 0.0551
R indices (all data)	R1 = 0.0405, wR2 = 0.1027	R1 = 0.0218, wR2 = 0.0567
extinction coeff	0.0010(10)	0.0015(4)
largest diff peak and hole (e Å^{-3})	0.479 and −0.353	0.306 and −0.307

[a] All data were collected on a SMART CCD diffractometer with Mo Kα radiation (λ = 0.710 73 Å). Data were refined using full-matrix least squares on F^2. No absorption correction was applied. [b] In this formula we assume D = H.

[i-PrNSN]$Zr(CH_2CHMe_2)_2$ is stable in solution at room temperature for several hours and can be heated to 80 °C for a few minutes before a small degree of decomposition is detected (by ^{1}H NMR). Interestingly, we have not been able to prepare [i-PrNSN]$Zr(CH_2CH_3)_2$ by analogous methods; presumably it is markedly less stable than [i-PrNSN]$Zr(CH_2CHMe_2)_2$, since the β protons in an ethyl complex are relatively accessible and subject to more rapid β abstraction.[10]

A single-crystal X-ray study of [t-BuNSN]ZrCl(NMe_2) (Figure 1; Tables 1 and 2) shows that it is approximately a trigonal bipyramid with the chloride and sulfur atoms in the axial positions (Cl−Zr−S angle 178.86(4)°), a *fac* geometry. In the ideal *fac* form, the angle between one N−Zr−S plane and the other would be ∼120°. In contrast, in an ideal *mer* form, the angle between one N−Zr−S plane and the other would be 180°. (As shown in eq 3, for a dialkyl complex *fac* and *mer* forms can be

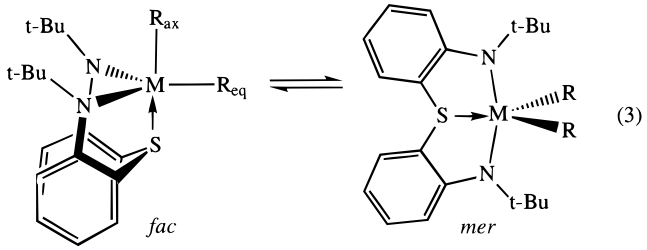

(3)

interconverted relatively easily by varying the N−Zr−N angle and rotating the MR_2 unit in the MR_2S plane.) In [t-BuNSN]ZrCl(NMe_2) the angle between the N(1)−Zr−S and N(2)−Zr−S planes is 117°. The "equatorial" angles at Zr sum to 343.17° and are not equal, with the largest (N(1)−Zr−N(3) = 124.08(13)°) being approximately 20° larger than the other two. The ligand backbone also is twisted (in Figure 1b, the twist is clockwise if viewed down the Cl−Zr−S vector); i.e., the *tert*-butyl group that contains C(201) points toward N(1)

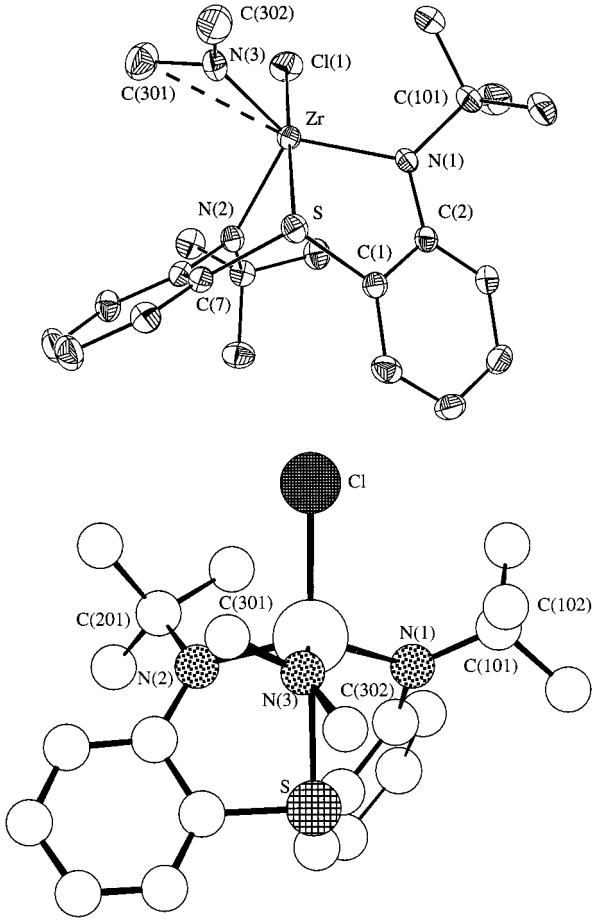

Figure 1. (a, top) ORTEP drawing of the structure of [t-BuNSN]ZrCl(NMe_2): N(3)−C(302) = 1.406(6) Å, N(3)−C(301) = 1.435(6) Å, Zr−C(301) = 2.849(5) Å, Zr−N(3)−C(302) = 136.4(3)°, Zr−N(3)−C(301) = 107.9(3)°. (b, bottom) Side view of a Chem 3D drawing of the structure of [t-BuNSN]ZrCl(NMe_2).

and the *tert*-butyl group that contains C(101) points toward N(3). Steric interaction between the *tert*-butyl group that contains C(101) and the NMe_2 ligand is likely

(10) Negishi, E.; Takahashi, T. *Acc. Chem. Res.* **1994**, *27*, 124.

Table 2. Selected Bond Lengths (Å) and Angles (deg) in [t-BuNSN]ZrCl(NMe$_2$), [i-PrNSN]ZrMe$_2$, and [t-BuNON]ZrMe[MeB(C$_6$F$_5$)$_3$]

[t-BuNSN]ZrCl(NMe$_2$)		[i-PrNSN]ZrMe$_2$		[t-BuNON]ZrMe[MeB(C$_6$F$_5$)$_3$][a]	
Zr−S	2.7273(10)	Zr−S	2.7343(9)	Zr−O	2.256
Zr−N(1)	2.102(3)	Zr−N(1)	2.088(2)	Zr−N(1)	2.049(10)
Zr−N(2)	2.098(3)	Zr−N(2)	2.133(2)	Zr−N(2)	2.065(10)
Zr−Cl(1)	2.4555(11)	Zr−C(1)	2.245(3)	Zr−C(1)	2.487(12)[b]
Zr−N(3)	2.059(3)	Zr−C(2)	2.250(3)	Zr−C(2)	2.200(13)
N(1)−Zr−N(2)	109.91(12)	N(1)−Zr−N(2)	135.66(8)	N(1)−Zr−N(2)	113.8(4)
N(1)−Zr−S	72.22(9)	N(1)−Zr−S	72.20(6)	N(1)−Zr−O	73.5(4)
N(1)−Zr−Cl(1)	107.04(9)	N(1)−Zr−C(1)	102.67(10)	N(1)−Zr−C(1)	118.6(5)
N(1)−Zr−N(3)	124.08(13)	N(1)−Zr−C(2)	99.64(10)	N(1)−Zr−C(2)	113.8(5)
N(2)−Zr−S	75.12(9)	N(2)−Zr−S	71.26(7)	N(2)−Zr−O	75.2(3)
N(2)−Zr−Cl(1)	106.00(9)	N(2)−Zr−C(1)	112.71(10)	N(2)−Zr−C(1)	101.2(5)
N(2)−Zr−N(3)	109.18(12)	N(2)−Zr−C(2)	89.04(11)	N(2)−Zr−C(2)	115.4(5)
N(3)−Zr−S	81.10(9)	C(2)−Zr−S	135.06(10)	C(2)−Zr−O	79.2(4)
N(3)−Zr−Cl(1)	98.70(10)	C(2)−Zr−C(1)	115.11(12)	C(2)−Zr−C(1)	91.8(5)
Cl(1)−Zr-S	178.86(4)	C(1)−Zr-S	109.77(8)	C(1)−Zr-O	167.3(4)
C(7)−S-C(1)	106.1(2)	C(21)−S-C(11)	103.51(13)	C−O−C	116.4(11)
Zr−N(1)−C(101)	122.9(2)	Zr−N(1)−C(17)	104.1(2)	Zr−N(2)−C(27)	129.3(8)
Zr−N(2)−C(201)	123.7(2)	Zr−N(2)−C(27)	121.3(2)	Zr−N(1)−C(17)	125.8(7)
N(1)/Zr/S/N(2)[c,d]	117	N(1)/Zr/S/N(2)[c,d]	154	N(1)/Zr/O/N(2)[c,d]	121
S−Zr−N(1)−C(1)[d]	140.3	S−Zr−N(1)−C(17)[d]	170.9	O−Zr−N(1)−C(1)[d]	140.3
S−Zr−N(2)−C(2)[d]	134.9	S−Zr−N(2)−C(27)[d]	164.7	O−Zr−N(1)−C(1)[d]	129.3

[a] See ref 1. [b] Methyl group bridging between Zr and B. [c] The external angle between the planes. [d] Obtained from Chem 3D model.

to give rise to the relatively large N(1)−Zr−N(3) angle and also to the C(301)−N−C(302) plane being twisted approximately halfway between an orientation parallel to the N(1)/N(2)/N(3) plane and one perpendicular to the N(1)/N(2)/N(3) plane (C(302)−N(3)−Zr−S = 48°). (The closest H···H contact between a proton attached to C(302) and one attached to C(102) in the structure is ∼2.4 Å, whereas if the C(301)−N−C(302) plane is perpendicular to the Cl−Zr−S axis, with no other changes, the closest H···H contact is ∼1.9 Å, according to a Chem 3D model.) There is also evidence for a weak agostic[11] Zr−C(301) interaction (2.849 Å), according to bond angles and distances in the Zr−NMe$_2$ group, in particular Zr−C(301) = 2.849(5) Å and Zr−N(3)−C(301) = 107.9(3)°. A weak agostic-like interaction may be possible as a consequence of steric hindrance that already distorts the dimethylamido group in the observed direction. The Zr−N bond lengths are similar to those expected for Zr−amido complexes (2.05−2.12 Å),[1,4,7,12−14] and the sum of the angles at each amido nitrogen atom is 360° (within 3σ). The zirconium−sulfur bond length (2.7273(10) Å) is similar to that (2.730(4) Å) reported for [Cp*$_2$ZrMe(THT)]$^+$[BPh$_4$]$^-$ (THT = tetrahydrothiophene)[15] or that (2.8046(9) Å) reported for [(2,6-Me$_2$C$_6$H$_3$NCH$_2$CH$_2$)$_2$S]ZrMe$_2$.[7] Finally, the angle at sulfur (106.1(2)°) is slightly larger than the corresponding angle in titanium complexes that contain the substituted [(O-*o*-C$_6$H$_4$)$_2$S]$^{2-}$ ligand[16−20] (e.g., 100.8(2)° in [(O-2,4-Me$_2$-*o*-C$_6$H$_4$)$_2$S]Ti(O−i-Pr)$_2$[19]) but approximately the same as the angle found in [(2,6-Me$_2$C$_6$H$_3$-NCH$_2$CH$_2$)$_2$S]ZrMe$_2$ (105.0(2)°).[7]

A single-crystal X-ray study of [i-PrNSN]ZrMe$_2$ (Figure 2; Tables 1 and 2) shows it to have a structure that is approximately halfway between a *fac* and an ideal *mer* geometry, as judged by the N(1)/Zr/S/N(2) value (angle between the N(1)−Zr−S and N(2)−Zr−S planes) of 154°. The view in Figure 2b emphasizes the approximately square-pyramidal core in which N(1)−Zr−N(2) and C(2)−Zr−S are equal (135°) and the angles between C(1) and the four "equatorial" atoms vary from 102.67° (N(1)−Zr−C(1)) to 115.11° (C(2)−Zr−C(1)). The S−Zr−N−C dihedral angles are relatively large compared to what they are in [t-BuNSN]ZrCl(NMe$_2$). However, the C−S−C angles are similar in the two complexes, as are the Zr−S and Zr−N$_{amido}$ bond distances. A curious feature of the structure of [i-PrNSN]ZrMe$_2$ is the fact that although the angles around N(1) sum to 360.0° (Zr−N(1)−C(17) = 104.1° Zr−N(1)−C(16) = 132.9°, and C(17)−N(1)−C(16) = 123.0°), as is the case in all diamido/donor complexes we have examined to date, the angles around N(2) sum to 346.6° (Zr−N(2)−C(27) = 121.3°, Zr−N(2)−C(26) = 108.1°, and C(27)−N(1)-C(26) = 117.2°); i.e., N(2) is markedly distorted from planarity. The slightly longer Zr−N(2) bond distance (2.088(2) Å) *may* be a reflection of a somewhat weaker π bond between Zr and N(2) as a consequence of the nonplanarity of N(2). Consistent with a weaker Zr−N(2) π bond is the relatively large difference between the two Zr−N$_{amido}$ bond lengths in [i-PrNSN]-ZrMe$_2$ (0.045 Å) compared to the difference in [t-BuNSN]-ZrCl(NMe$_2$) (0.004 Å).

Solution proton and carbon NMR spectra of [t-BuNSN]Zr(NMe$_2$)$_2$ and [t-BuNSN]ZrMe$_2$ suggest that structures which contain two inequivalent NMe$_2$ and methyl

(11) Brookhart, M.; Green, M. L. H.; Wong, L. *Prog. Inorg. Chem.* **1988**, *36*, 1.
(12) Guérin, F.; McConville, D. H.; Vittal, J. J. *Organometallics* **1996**, *15*, 5586.
(13) Aoyagi, K.; Gantzel, P. K.; Kalai, K.; Tilley, T. D. *Organometallics* **1996**, *15*, 923.
(14) Schrock, R. R.; Seidel, S. W.; Schrodi, Y.; Davis, W. M. *Organometallics* **1999**, *18*, 428.
(15) Eshuis, J. J.; Tan, Y. Y.; Meetsma, A.; Teuben, J. H.; Renkema, J.; Evens, G. G. *Organometallics* **1992**, *11*, 362.
(16) Miyatake, T.; Mizunuma, K.; Seki, Y.; Kakugo, M. *Makromol. Chem. Rapid Commun.* **1989**, *10*, 349.
(17) Miyatake, T.; Mizunuma, K.; Kakugo, M. *Makromol. Chem. Macromol. Symp.* **1993**, *66*, 203.
(18) van der Linden, A.; Schaverien, C. J.; Meijboom, N.; Ganter, C.; Orpen, A. G. *J. Am. Chem. Soc.* **1995**, *117*, 3008.
(19) Fokken, S.; Spaniol, T. P.; Kang, H.-C.; Massa, W.; Okuda, J. *Organometallics* **1996**, *15*, 5069.
(20) Porri, L.; Ripa, A.; Colombo, P.; Miano, E.; Capelli, S.; Meille, S. V. *J. Organomet. Chem.* **1996**, *514*, 213.

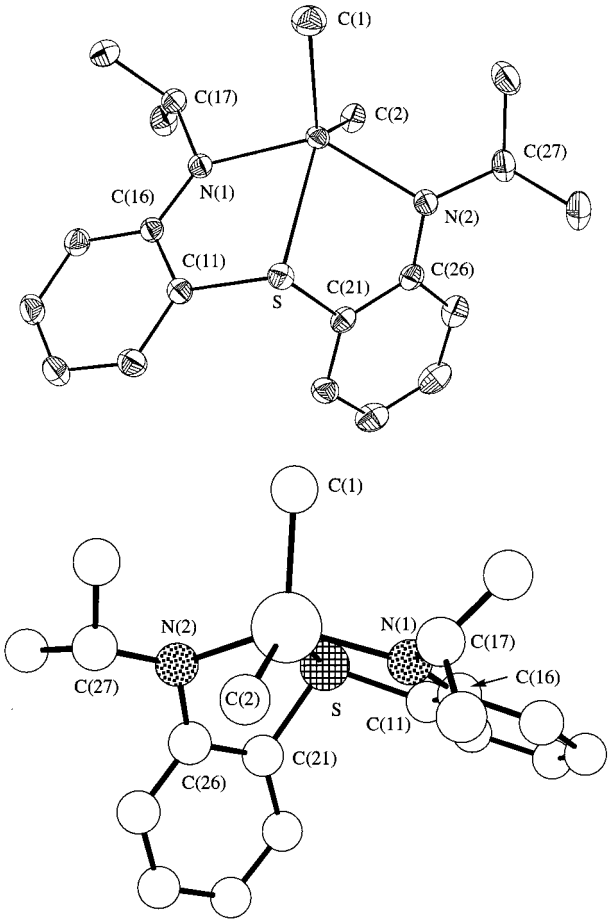

Figure 2. (a, top) ORTEP drawing of the structure of [i-PrNSN]$ZrMe_2$. (b, bottom) Side view of a Chem 3D drawing of the structure of [i-PrNSN]$ZrMe_2$.

groups, respectively, presumably "twisted" *fac* structures analogous to the structure of [t-BuNSN]ZrCl(NMe_2), can be observed at low temperatures and that the inequivalent NMe_2 or Me groups interconvert rapidly on the NMR time scale at higher temperatures. For example, in the ^{1}H NMR spectrum of [t-BuNSN]$ZrMe_2$ (Figure 3) at 0 °C a single *tert*-butyl resonance,

Table 3. Variable-Temperature ^{1}H NMR Studies of Fluxional $[RNSN]^{2-}$ Complexes

	$\Delta\nu$ (±2 Hz)[a]	resonance	T_c (±2 K)	$\Delta G_c^{\ddagger}$ (kcal/mol)[b]
[t-BuNSN]$Zr(NMe_2)_2$	152	NMe_2	259	12.1
	162	t-Bu	223	10.3[c]
[t-BuNSN]$ZrMe_2$	20	Zr−Me	243	12.3
	100	t-Bu	208	9.8[c]
[i-PrNSN]$Zr(NMe_2)_2$	79	NMe_2	342	16.6
	52	$CHMe_2$	337	16.7
[i-PrNSN]$ZrMe_2$	180	Zr−Me	319	14.9
	205	$CHMe_2$	320	14.9
[i-PrNSN]$Zr(CH_2CHMe_2)_2$	134	CH_2CHMe_2	323	15.3
	190	$CHMe_2$	319	14.9

[a] Estimated from resolved spectra at lower temperature. [b] Calculated using the estimated value of $\Delta\nu$. Error (σ) estimated to be ±0.1. [c] Ascribed to a freezing out of the fac_{C1} conformation.

a single methyl resonance, and four aromatic backbone resonances are observed, consistent with a *mer* structure on the NMR time scale, either the ideal *mer* structure (with C_{2v} symmetry) or the more likely "twisted" form (with C_2 symmetry) in which the *tert*-butyl carbon atoms do not lie in the MN_2S plane. As the sample is cooled, the average resonance for the two methyl groups on the metal becomes two at approximately −30 °C. When the sample of [t-BuNSN]$ZrMe_2$ is cooled further, the two *tert*-butyl groups become inequivalent and yield two broad resonances, while more than four aromatic proton resonances can be seen. In the −78 °C spectrum only one of the two broad *tert*-butyl resonances is visible at 1.4 ppm; the broader of the two *tert*-butyl resonances is buried under the resonances for the two methyl groups near 1 ppm. These data are consistent with a "twisted" *fac* (fac_{C1}) form analogous to what is found in the solid state for [t-BuNSN]ZrCl(NMe_2) at the lowest temperature. The fact that the *tert*-butyl resonances are broad, and one is much broader than the other, suggests that rotation of the *tert*-butyl groups is being restricted in the fac_{C1} structure, and more so in one *tert*-butyl group than the other. The two *tert*-butyl groups and all eight aryl protons would be inequivalent in a fac_{C1} structure. All eight aryl proton resonances cannot be resolved, although more than four different kinds of aryl proton

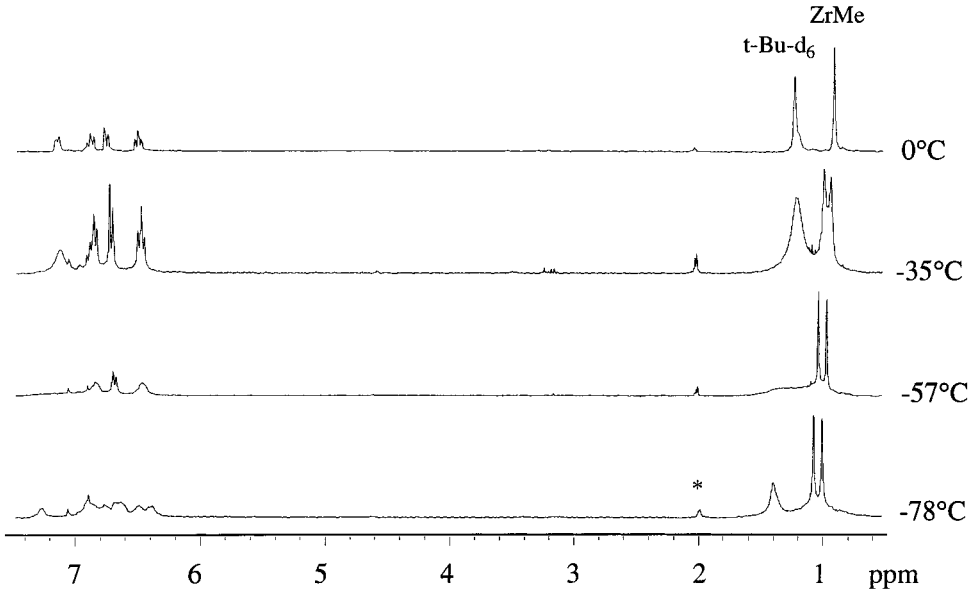

Figure 3. Variable-temperature proton NMR (300 MHz) of [t-BuNSN]$ZrMe_2$ in toluene-d_8 (*).

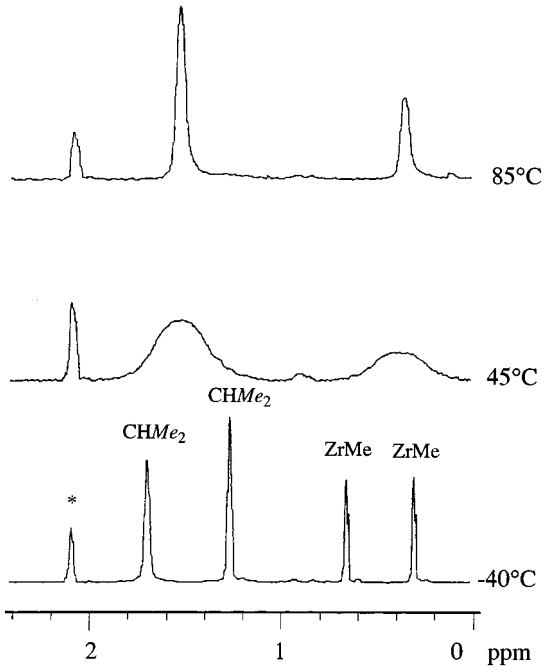

Figure 4. Variable-temperature proton NMR (500 MHz) of [i-PrNSN]$ZrMe_2$ in toluene-d_8 (*).

resonances clearly are present in the spectrum at −78 °C. The variable-temperature ^{13}C NMR spectrum of [t-BuNSN]$Zr(^{13}CH_3)_2$ showed ^{13}C resonances at 45.89 and 44.50 ppm at −30 °C that coalesced at −10 °C. Similar spectra are observed for [t-BuNSN]$Zr(NMe_2)_2$, and activation barriers for two different processes can be observed. The barriers for each of these processes in [t-BuNSN]$Zr(NMe_2)_2$ and [t-BuNSN]$ZrMe_2$ are listed in Table 3. The process in which *fac* and *mer* forms interconvert has a value for $\Delta G_c^{\ddagger}$ of ∼12 kcal/mol at the coalescence temperature, while $\Delta G_c^{\ddagger}$ for the twisting process within the *fac* form is ∼10 kcal/mol for both [t-BuNSN]$Zr(NMe_2)_2$ and [t-BuNSN]$ZrMe_2$. It cannot be determined if the *mer* transition state has C_{2v} or C_2 symmetry, but in either case the sulfur must actually invert through a planar form.

The NMR spectrum of [i-PrNSN]$ZrMe_2$ at −40 °C (Figure 4) reveals resonances for two inequivalent methyl groups on Zr at 0.32 and 0.67 ppm and resonances for two types of isopropyl methyl groups at 1.27 and 1.64 ppm, consistent with the square-pyramidal structure found in the solid state. On the basis of the fact that only four types of aryl proton resonances and one type of methine resonance are observed at −78 °C, the square-pyramidal structure apparently has a plane of symmetry on the NMR time scale at that temperature. However, the isopropyl methyl resonances at 1.27 and 1.64 ppm are not sharp doublets, which could be taken as evidence that a lower symmetry (e.g., twisted) form is actually observable on the NMR time scale in this case also but that differences in chemical shifts are relatively small. What is clear, however, is that upon warming the sample, the axial and equatorial methyl groups interconvert and the isopropyl methyl groups interconvert, essentially at the same rate (∼15 kcal/mol; Figure 4 and Table 3). Similar spectra are observed for [i-PrNSN]$Zr(NMe_2)_2$ and [i-PrNSN]$Zr(CH_2CHMe_2)_2$. All data are consistent with inversion at sulfur via a *mer* form. As shown in Table 3, the values for $\Delta G_c^{\ddagger}$ for inversion at sulfur in the [i-PrNSN]$^{2-}$ structures vary between 15 and 17 kcal/mol, a few kcal/mol higher than the $\Delta G_c^{\ddagger}$ values for inversion at sulfur in the [t-BuNON]$^{2-}$ structures. The fact that the $\Delta G_c^{\ddagger}$ values for inversion at sulfur in the [t-BuNSN]$^{2-}$ and [i-PrNSN]$^{2-}$ complexes do not differ greatly suggests that inversion is the rate-limiting process in each case and that steric differences between *tert*-butyl and isopropyl groups have only a small effect.

Cationic Zirconium Complexes Containing [t-BuNSN]$^{2-}$ and [i-PrNSN]$^{2-}$. Reaction of [t-BuNSN]$ZrMe_2$ and 1 equiv of $[Ph_3C][B(C_6F_5)_4]$ in chlorobenzene-d_5 at −30 °C leads to a color change from red-orange to yellow-orange. The proton and carbon NMR spectra of the resulting species in solution are indicative of clean methyl abstraction to give Ph_3CMe and "{[t-BuNSN]ZrMe}$\{B(C_6F_5)_4\}$". In "{[t-BuNSN]ZrMe}$\{B(C_6F_5)_4\}$" are found a Zr−Me resonance at 1.09 ppm and a broadened resonance for the ^{13}C-labeled methyl group at 52.78 ppm (cf. 0.72 and 53.60 ppm in "{[t-BuNON]ZrMe}$\{B(C_6F_5)_4\}$" in C_6D_5Br[9]). In chlorobenzene, the cation decomposes within minutes at room temperature but it is relatively stable at lower temperatures (∼1 h at 0 °C; 2−3 h at −10 °C). The stability of the cation in bromobenzene is lower, so that some decomposition is observed within 30 min at 0 °C. We also attempted to synthesize the base adduct {[t-BuNSN]ZrMe$(PhNMe_2)$}$\{B(C_6F_5)_4\}$ in the hope of making a more stable cation. For example, 1 or 2 equiv of $PhNMe_2$ was added to a −30 °C solution of "{[t-BuNSN]ZrMe}$\{B(C_6F_5)_4\}$" (prepared by methyl abstraction with $[Ph_3C]^+$). The desired base adduct appeared to form initially, but complete decomposition was observed within 3 h at −30 °C. In contrast, addition of THF (3 equiv) to {[t-BuNSN]ZrMe$(PhNMe_2)$}$\{B(C_6F_5)_4\}$ led to clean formation of {[t-BuNSN]ZrMe$(THF)_x$}$\{B(C_6F_5)_4\}$ that has no symmetry on the NMR time scale at room temperature. The THF adduct is stable at room temperature for 10−15 min (and for hours at lower temperatures) before it begins to decompose.

Attempts to prepare cationic complexes from [i-PrNSN]$ZrMe_2$ and [i-PrNSN]$Zr(CH_2CHMe_2)_2$ were analogous to methods used to prepare cations from [t-BuNSN]$ZrMe_2$. Reaction of equimolar amounts of [i-PrNSN]$ZrMe_2$ (or [i-PrNSN]$Zr(CH_2CHMe_2)_2$) and $[Ph_3C][B(C_6F_5)_4]$ in chlorobenzene-d_5 at −30 °C led to decomposition (according to ^1H NMR spectra) along with a color change to deep red. Formation of cations via protonation reactions was only slightly more successful. $[PhNHMe_2][B(C_6F_5)_4]$ was added to a −30 °C solution of [i-PrNSN]$ZrMe_2$, and when the solution was warmed to −10 °C for 45 min or ∼23 °C for 15 min, the color changed from pale yellow to orange. The ^1H NMR of the reactions under various conditions was indicative of at least two main species (**A** and **B**, see Experimental Section) having been formed, as evidenced by two methine resonances at 4.0−3.0 ppm and two pairs of isopropyl methyl resonances at 1.6−0.6 ppm. A bromobenzene-d_5 solution containing an equimolar mixture of $[PhNHMe_2][B(C_6F_5)_4]$ and [i-PrNSN]$ZrMe_2$ was warmed from ∼−30 °C to ∼23 °C as the reaction was monitored by ^1H NMR. Protonation of the methyl group and production of methane was observed as species **A** (∼80%) and species **B** (∼20%) were formed initially.

Over the next 30−40 min, species **B** increased in concentration at the expense of **A** and the solution turned dark red. Appreciable decomposition was observed within 60 min, with complete decomposition occurring in ∼2 h. We believe that **A** is the desired cation, {[i-PrNSN]ZrMe(PhNMe$_2$)}{B(C$_6$F$_5$)$_4$}; the identity of species **B**, into which **A** apparently is transformed, is unknown. Reaction of [PhNHMe$_2$][B(C$_6$F$_5$)$_4$] and [i-PrNSN]ZrMe$_2$ in the presence of an extra 1 equiv of PhNMe$_2$ does not further stabilize the cation; decomposition is observed within 20 min at room temperature. Attempts were also made to trap a clean base adduct of species **A** by performing the reaction in the presence of 3−4 equiv of THF. The ^{1}H NMR of the resulting reaction was indicative of a mixture of THF-solvated complexes. Finally, reaction of [PhNHMe$_2$][B(C$_6$F$_5$)$_4$] and [i-PrNSN]Zr(CH$_2$CHMe$_2$)$_2$ under a variety of reaction conditions gave a complex mixture of products (^{1}H NMR).

When 1-hexene was added to "{[t-BuNSN]ZrMe}{B(C$_6$F$_5$)$_4$}" (generated in chlorobenzene at −10 °C from [t-BuNSN]ZrMe$_2$ and [Ph$_3$C][B(C$_6$F$_5$)$_4$]), oligomerization of 1-hexene was observed, but no polymerization to any significant extent. (Approximately 20 equiv of 1-hexene was consumed within the lifetime (∼3 h) of the initiator at −10 °C.) It is not clear whether this low degree of polymerization is due to inherently slow propagation or to a thermal instability of the cationic initiator and the intermediate cation that contains the growing polymer chain. This behavior differs markedly from that found for "{[t-BuNON]ZrMe}{B(C$_6$F$_5$)$_4$}", which is a living catalyst for the polymerization of 1-hexene at 0 °C in chlorobenzene.[2]

Discussion

The structure of [t-BuNSN]ZrCl(NMe$_2$) is similar to that of [t-BuNON]ZrMe[MeB(C$_6$F$_5$)$_3$], although there are some notable, but understandable, differences (Table 2).[1] The Zr−S bond is nearly 0.5 Å longer than the Zr−O bond in [t-BuNON]ZrMe[MeB(C$_6$F$_5$)$_3$], a difference that is expected on the difference in the van der Waals radii[21] of an oxygen in a typical ether (1.4−1.6 Å) and a sulfur in a typical thioether (1.8−1.9 Å). The external angle between the N(1)−S−Zr and N(2)−S−Zr planes (117°) in [t-BuNSN]ZrCl(NMe$_2$) is ∼4° less than the corresponding angle in [t-BuNON]ZrMe[MeB(C$_6$F$_5$)$_3$] (121°). The C$_{ipso}$−S−C$_{ipso}$ angle (106.1(2)°) is ∼10° smaller in [t-BuNSN]ZrCl(NMe$_2$) than the C$_{ipso}$−O−C$_{ipso}$ angle in [t-BuNON]ZrMe[MeB(C$_6$F$_5$)$_3$] (116.4(9)°), which is a typical difference in an angle at sulfur versus oxygen (e.g., H−S−H = 92.1° and H−O−H = 104.5° in the gas phase[22]). Finally, the N−M−N angle (109.91(12)°) is ∼4° smaller in [t-BuNSN]ZrCl(NMe$_2$) than in [t-BuNON]ZrMe[MeB(C$_6$F$_5$)$_3$].[1] The X−M−N(1)−C(1) dihedral angles (X = O, S) are approximately the same in [t-BuNSN]ZrCl(NMe$_2$) and [t-BuNON]ZrMe[MeB(C$_6$F$_5$)$_3$], although the M−N−C angles appear to be several degrees *smaller* in [t-BuNSN]ZrCl(NMe$_2$). The C$_{ipso}$−S−C$_{ipso}$ angle appears to be restricted, which leads to some decrease in the external angle between the N(1)−S−Zr and N(2)−S−Zr planes and the N(1)−M−N(2) angle, compared to [t-BuNON]$^{2-}$ complexes. Smaller Zr−N−C angles in [t-BuNSN]ZrCl(NMe$_2$) (by ∼5°) would seem likely to exacerbate steric crowding near the *tert*-butyl groups.

In contrast, the structures of [i-PrNSN]ZrMe$_2$ and [i-PrNON]ZrMe$_2$[23] are significantly different. Compound [i-PrNON]ZrMe$_2$ has a "twisted" *mer* (C_2) structure with an "S-shaped" backbone. The "equatorial" methyl groups therefore are interconverted in a C_2 operation. The oxygen donor is strictly planar. In [i-PrNSN]ZrMe$_2$ the analogous *mer* form is higher in energy than the observed square-planar form as a consequence of the "fixed" C−S−C angle and the reluctance of sulfur to adopt sp^2 hybridization and therefore the required trigonal-planar geometry at sulfur. We believe that the structure of [i-PrNSN]ZrMe$_2$ is not analogous to that of [t-BuNSN]ZrMe$_2$ as a consequence of a lower degree of steric interaction between the i-Pr groups and the methyl groups than between the t-Bu groups and the methyl groups, and that t-Bu/methyl interactions in the case of [t-BuNSN]ZrMe$_2$ provides additional impetus for forming a *fac*$_{C1}$ geometry. The ground-state structure of [i-PrNSN]ZrMe$_2$ therefore is approximately a square pyramid, a structure approximately halfway between a *fac* and a *mer* form.

The difference in the thermal stabilities of [t-BuNSN]ZrMe$_2$ and [i-PrNSN]ZrR$_2$ species (R = Me, CH$_2$CHMe$_2$) is striking. We hypothesize that five-coordinate complexes that contain the [t-BuNSN]$^{2-}$ ligand are sterically more crowded in subtle but significant ways than complexes that contain the [i-PrNSN]$^{2-}$ ligand and that steric crowding leads to decomposition of [t-BuNSN]$^{2-}$ complexes. A decomposition pathway unique to a *tert*-butyl-substituted neutral complex would be loss of a *tert*-butyl radical, a process that has been documented in diamido/phosphorus donor systems recently.[14] Cleavage of an aryl−sulfur bond in either a [t-BuNSN]$^{2-}$ or a [i-PrNSN]$^{2-}$ complex also seems plausible in view of the recently documented cleavage of an aryl−oxygen bond in a proposed [i-PrNON]Ti^{II} intermediate.[9] It is also striking that many more [t-BuNON]ZrR$_2$ complexes (including R = CH$_2$CHMe$_2$) can be prepared than [t-BuNSN]ZrR$_2$ complexes, although there appear to be steric limitations in the [t-BuNON]ZrR$_2$ system also (e.g., R apparently cannot be CH$_2$CMe$_3$).[9] Although it is tempting to propose that some modes of decomposition might be faster as a consequence of sulfur being more electron donating (in a σ sense) than oxygen, there are no quantitative or even semiquantitative data that result from this work that would support such an assertion.

The finding that activated [t-BuNON]ZrMe$_2$ is an initiator for the living polymerization of 1-hexene contrasts with the finding that activated [i-PrNON]ZrMe$_2$ will only oligomerize 1-hexene.[24] Nevertheless, both initiators appear to be stable at room temperature. The fact that neither [t-BuNSN]ZrMe$_2$ nor [i-PrNSN]ZrMe$_2$ can be activated to yield stable initiators that will oligomerize or polymerize 1-hexene under analogous conditions raises suspicion that modes of decomposition might be operative that can be traced *directly* to sulfur.

(21) Bondi, A. *J. Phys. Chem.* **1964**, *68*, 441.
(22) Greenwood, N. N.; Earnshaw, A. *Chemistry of the Elements*; Pergamon: Oxford, U.K., 1984.
(23) Baumann, R.; Davis, W. M.; Schrock, R. R., submitted for publication.
(24) Liang, L.-C.; Schrock, R. R., unpublished results.

However, we cannot say conclusively that this is the case. It should be noted that cations prepared by activation of $[(ArylNCH_2CH_2)_2S]ZrMe_2$ also did not appear to be as stable as those prepared by activation of $[(ArylNCH_2CH_2)_2O]ZrMe_2$,[7] although the consequences of any decomposition reaction again could not be documented. Finally, we note that titanium complexes that contain the $[(O\text{-}o\text{-}C_6H_4)_2S]^{2-}$ ligand[16−20] have been prepared and evaluated as precursors to polymerization catalysts, but no well-behaved polymerization activity has yet been reported.

Conclusions

The thioethers (t-Bu-d_6-NH-o-$C_6H_4)_2S$ and (i-PrNH-o-$C_6H_4)_2S$ can be prepared readily and employed to prepare some zirconium dialkyl complexes via [RNSN]-$Zr(NMe_2)_2$ and [RNSN]$ZrCl_2$ intermediates. [i-PrNSN]-ZrR_2 (R = Me, CH_2CHCMe_2) complexes are significantly more stable than [t-BuNSN]$ZrMe_2$, perhaps because of some exacerbated steric hindrance and concomitant weakness of the t-Bu−N bond or $S-C_{ipso}$ bond in such circumstances. Inversion at sulfur in five-coordinate dialkyl complexes is significantly slower than inversion at oxygen in analogous complexes that contain the $[t\text{-BuNON}]^{2-}$ ligand. Cationic complexes prepared from $[RNSN]ZrMe_2$ precursors were neither stable at 22 °C nor active initiators for the controlled polymerization of 1-hexene.

Experimental Section

General Considerations. Unless noted otherwise, all experiments were conducted under nitrogen in a Vacuum Atmospheres drybox or by using standard Schlenk techniques. Nitrogen (for Schlenk work) and ethylene gases were purified by passage through an activated, zeolite-supported MnO catalyst (BOC Gases). Toluene was distilled from sodium/benzophenone. Pentane, diethyl ether, and tetrahydrofuran were deoxygenated and dried by first sparging with nitrogen and then passing through either (a) two large activated alumina columns (diethyl ether and THF) or (b) one large activated alumina column and then one large column of activated Q5 (pentane).[25] Dichloromethane and chlorobenzene (Aldrich HPLC grade, 99.9%) were distilled from CaH_2 under nitrogen. Solvents were stored in the drybox over activated 4 Å sieves. 1-Hexene was refluxed over sodium for 4 days, distilled, and stored over activated 4 Å sieves. Molecular sieves and Celite were activated in vacuo (10^{-3} Torr) for 24 h at 175 and 125 °C, respectively.

Unless noted otherwise, ^1H and ^{13}C NMR spectra were recorded at 300 and 75 MHz, respectively. Chemical shifts were referenced using the residual solvent peak and are listed as parts per million downfield from tetramethylsilane. Routine coupling constants are not listed. All NMR spectra were recorded at room temperature unless noted otherwise. All NMR solvents were deoxygenated and dried over 4 Å sieves. Elemental analyses were performed with a Perkin-Elmer 2400 CHN analyzer or were carried out by Microlytics of Deerfield, MA. As this analysis measures the number of moles of water produced, the percentage of hydrogen for deuterium-containing compounds was calculated from the actual molecular weight, assuming that all ^2H present was actually ^1H.

$Zr(NMe_2)_4$[26] was prepared according to the literature procedure. $[Ph_3C][B(C_6F_5)_4]$ and $[PhNMe_2H][B(C_6F_5)_4]$ were gifts from Exxon Chemical Corp. Other reagents were purchased from commercial sources and used as received.

X-ray-quality crystals of [t-BuNSN]$ZrCl(NMe_2)$ were grown by cooling a concentrated diethyl ether solution. Crystals of [i-PrNSN]$ZrMe_2$ were obtained by cooling a diethyl ether/benzene solution. X-ray data were collected on a SMART/CCD diffractometer as described elsewhere.[27] (See Supporting Information for full details.)

S(o-$C_6H_4NO_2)_2$. To a vigorously stirred suspension of K_2CO_3 (71 g, 0.51 mol) in 500 mL of degassed DMSO were added o-$C_6H_4(NO_2)SH$[28] (40 g, 0.26 mol) and o-$C_6H_4(NO_2)F$ (36 g, 0.26 mol). After 18 h of stirring at room temperature, the solution was poured into 1.5 L of stirred ice/water and the yellow precipitate was collected by filtration. The precipitate was dried in vacuo at 60 °C for 12 h to give 72 g (100%) of S(o-$C_6H_4NO_2)_2$ as a yellow solid. The crude product was >95% pure (according to its ^1H NMR spectrum) and was used without further purification: ^1H NMR ($CDCl_3$) δ 8.09 (dd, 2), 7.48 (m, 4), 7.28 (d, 2); ^{13}C NMR ($CDCl_3$) δ 149.9, 134.2, 134.1, 132.1, 129.1, 126.0.

S(o-$C_6H_4NH_2)_2$. A 1 L hydrogenation vessel was charged with 10% Pd on carbon (3.5 g, 3.3 mmol of Pd), S(o-$C_6H_4NO_2)_2$ (70 g, 0.25 mol), and 600 mL of degassed 95% ethanol. The hydrogen vessel was purged three times with hydrogen gas, the pressure was adjusted to 60 psi, and the contents were heated to 80 °C for 48 h. The reaction mixture was cooled to ∼40 °C, and the suspension was filtered through a bed of Celite. The filtrate was concentrated in vacuo to about 200 mL and poured into 1.5 L of ice water. The white precipitate was collected by filtration, washed twice with 50 mL of water, and dried on a frit for ∼30 min. The solid was dissolved in dichloromethane, and the resulting solution was dried over $MgSO_4$. The mixture was filtered, and the filtrate was concentrated to about 75 mL. Hexane (500 mL) was added to the suspension, and the off-white solid was filtered off and washed twice with 10 mL of hexane. Concentration of the filtrate in vacuo yielded a second crop of solid: yield 49 g (91%); ^1H NMR ($CDCl_3$) δ 7.24 (dd, 2), 7.10 (td, 2), 6.71 (m, 4), 4.20 (br s, 4, NH_2); ^{13}C NMR ($CDCl_3$) δ 147.2, 133.9, 129.7, 119.5, 117.7, 116.0.

S[o-$C_6H_4NHC(CD_3)_2CH_3]_2$ (H_2[t-BuNSN]). S(o-$C_6H_4NH_2)_2$ (30.0 g, 0.139 mol) was dissolved in acetone-d_6 (90 g, 1.4 mo), and 50 g of activated 4 Å sieves was added. After the diimine had completely formed (in about 10 days as judged by ^1H NMR), the acetone-d_6 was decanted off. The sieves were soaked in 100 mL of diethyl ether, separated by filtration, and washed twice with 20 mL of diethyl ether. The acetone and ether solutions were combined and the volatile components removed in vacuo to give the diimine as a viscous red oil. A solution of the diimine in 100 mL of diethyl ether was added dropwise to 300 mL of MeLi (1.4 M in diethyl ether) at −78 °C. After 2 h, the yellow solution was warmed to room temperature and stirred for 16 h. The mixture was transferred by cannula into 500 mL of vigorously stirred ice/water. The organic layer was separated, and the aqueous layer was extracted twice with 150 mL of diethyl ether. The organic layer was dried over $MgSO_4$, and the solvents were removed in vacuo. The red viscous oil was dissolved in a minimum amount of pentane. Chromatography of the crude product on an alumina column (40 × 4.5 cm) provided H_2[t-BuNSN] after elution with 500 mL of pentane followed by 3:1 pentane/diethyl ether. Recovery of H_2-[t-BuNSN] was monitored by TLC (R_f = 0.9 on Al_2O_3 with 3:1 pentane/diethyl ether as eluent). Removal of solvents in vacuo gave analytically pure H_2[t-BuNSN] as a pale orange solid (22 g, 47%): ^1H NMR ($CDCl_3$) δ 7.25 (dd, 2), 7.15 (td, 2), 6.98 (dd, 2), 6.62 (td, 2), 4.49 (br s, 2, NH), 1.32 (s, 6, CCH_3(CD_3)$_2$); ^{13}C NMR ($CDCl_3$) δ 147.2, 134.0, 129.8, 119.1, 117.7, 114.9, 51.6,

(25) Pangborn, A. B.; Giardello, M. A.; Grubbs, R. H.; Rosen, R. K.; Timmers, F. J. *Organometallics* **1996**, *15*, 1518.
(26) Diamond, G. M.; Rodewald, S.; Jordan, R. F. *Organometallics* **1995**, *14*, 5.
(27) Rosenberger, C.; Schrock, R. R.; Davis, W. M. *Inorg. Chem.* **1997**, *36*, 123.
(28) Overman, L. E.; Smoot, J.; Overman, J. D. *Synthesis* **1974**, 59.

30.2, 29.7 (m, $CCH_3(CD_3)_2$). Anal. Calcd for $C_{20}H_{16}D_{12}N_2S$: C, 70.53; H, 8.29; N, 8.23. Found: C, 70.13; H, 8.01; N, 8.01.

S[*o*-$C_6H_4NHCH(CH_3)_2$]$_2$ (H_2[i-PrNSN]). Zinc dust (15 g, 0.23 mol), S(*o*-$C_6H_4NH_2)_2$ (5.0 g, 0.023 mol), and acetone (13 g, 0.23 mol) were added to 80 mL of glacial acetic acid. The mildly exothermic reaction was stirred at room temperature and judged (by ^{1}H NMR) to be complete in 48 h. The reaction slurry was poured into a vigorously stirred mixture of 160 mL of concentrated aqueous NH_3, 140 mL of ice/water, and 300 mL of diethyl ether. Once most of the solid had dissolved, the layers were separated and the aqueous layer was extracted twice with 100 mL of diethyl ether. The organic extracts were combined and dried over $MgSO_4$. The solution was concentrated to ~50 mL in vacuo. The product was purified by flash chromatography on an alumina column (8 × 3 cm) using diethyl ether as the eluent. The solvent was removed in vacuo and the dark orange oil dried in vacuo (30 mTorr, 3 h) to give 6.6 g (95%) of analytically pure H_2[i-PrNSN]. The oil crystallizes upon standing for several weeks at room temperature: ^{1}H NMR (C_6D_6) δ 7.39 (dd, 2), 7.02 (td, 2), 6.50 (td, 2), 6.42 (dd, 2), 4.51 (d, 2, N*H*), 3.26 (sept, 2), 0.83 (d, 12); ^{13}C NMR (C_6D_6) δ 147.8, 134.5, 129.9, 117.4, 117.2, 111.6, 44.2 (NCH-(CH_3)$_2$), 22.8 (N*C*H(CH_3)$_2$). Anal. Calcd for $C_{18}H_{24}N_2S$: C, 71.96; H, 8.05; N, 9.32. Found: C, 71.70; H, 8.07; N, 9.33.

[t-BuNSN]Zr(NMe$_2$)$_2$. A solution of H_2[t-BuNSN] (4.00 g, 11.7 mmol) and $Zr(NMe_2)_4$ (3.14 g, 11.7 mmol) in 30 mL of toluene was heated to 65 °C under a slow purge of nitrogen. After 2 h, the reaction was carefully subjected to vacuum for ~10 s and backfilled with nitrogen three times. After 6, 10, and 16 h, the vacuum/backfill procedure was repeated. After 18 h at 65 °C, the toluene solution was cooled to room temperature, filtered, and concentrated to about 5 mL in vacuo. Pentane was added (10 mL) and the solution was cooled to −30 °C overnight. A first crop (3.60 g) of analytically pure colorless crystals of [t-BuNSN]Zr(NMe$_2$)$_2$ was isolated, washed with cold pentane, and dried in vacuo. A second crop (0.86 g) and third crop (0.22 g) of crystals were obtained from the filtrate by removal of all volatile components in vacuo and recrystallization of the residue from pentane: total yield (three crops) 4.68 g (77%); ^{1}H NMR (C_6D_6) δ 7.31 (dd, 2), 6.97 (m, 4), 6.62 (m, 2), 3.03 (s, 12, N(C*H*$_3$)$_2$), 1.16 (s, 6, CC*H*$_3$(CD_3)$_2$); ^{13}C NMR (C_6D_6) δ 154.7, 133.1, 129.8, 126.9, 126.6, 122.0, 58.3, 44.9, 32.2, 31.6 (m, $CCH_3(CD_3)_2$). Anal. Calcd for $C_{24}H_{26}D_{12}N_4SZr$: C, 55.79; H, 7.40; N, 10.85. Found: C, 55.74; H, 7.10; N, 10.78.

[t-BuNSN]ZrCl(NMe$_2$). Me_3SiCl (100 mg, 0.92 mmol) was added to a solution of [t-BuNSN]Zr(NMe$_2$)$_2$ (0.50 g, 0.97 mmol) in 15 mL of diethyl ether over a period of 5 min. The solution turned yellow and became cloudy. After 18 h, the suspension was concentrated to 8 mL and cooled to −30 °C overnight. The microcrystalline yellow solid was collected by filtration, washed twice with 1 mL of cold diethyl ether, and dried in vacuo (290 mg). A second crop (100 mg) was obtained by concentrating the filtrate to 3 mL and cooling (−30 °C) overnight. Total yield: 0.39 g (74%). Analytically pure samples were obtained by a second recrystallization from diethyl ether: ^{1}H NMR (C_6D_6) δ 7.21 (dd, 2), 6.94 (td, 2), 6.85 (dd, 2), 6.54 (td, 2), 2.97 (s, 6, N(C*H*$_3$)$_2$), 1.36 (s, 6, CC*H*$_3$(CD_3)$_2$); ^{13}C NMR (C_6D_6) δ 155.0, 151.9, 133.4, 130.4, 123.2, 121.8, 66.2, 43.3, 31.1, 30.4 (m, $CCH_3(CD_3)_2$). Anal. Calcd for $C_{22}H_{20}D_{12}ClN_3SZr$: C, 52.00; H, 6.35; N, 8.27. Found: C, 51.87; H, 6.35; N, 8.01.

[t-BuNSN]ZrCl$_2$. Me_3SiCl (3.8 g, 35 mmol) was added to a solution of [t-BuNSN]Zr(NMe$_2$)$_2$ (4.5 g, 8.7 mmol) in 50 mL of diethyl ether. Immediately a yellow color was observed, followed by precipitation of a bright yellow solid. After 12 h, the volatiles were removed in vacuo and 30 mL of pentane was added to the residue. The solid was filtered off, washed liberally with pentane, and dried in vacuo to give 4.1 g (94%) of crude product that was pure enough (>95% by NMR) for use in subsequent reactions. Analytically pure samples were obtained by recrystallization from toluene/pentane at −30 °C: ^{1}H NMR (C_6D_6) δ 7.05 (br m, 2), 6.81 (td, 2), 6.63 (dd, 2), 6.51 (td, 2), 1.22 (s, 6, CC*H*$_3$(CD_3)$_2$); ^{13}C NMR (C_6D_6, 70 °C) δ 153.2, 133.4, 130.9, 125.4, 123.9, 123.4, 59.2, 30.5, 29.9 (m, $CCH_3(CD_3)_2$). Anal. Calcd for $C_{20}H_{14}D_{12}Cl_2N_2SZr$: C, 48.09; H, 5.25; N, 5.61. Found: C, 48.05; H, 5.34; N, 5.44.

[t-BuNSN]ZrMe$_2$. To a precooled (−30 °C) suspension of [t-BuNSN]$ZrCl_2$ (0.85 g, 1.7 mmol) in 35 mL of diethyl ether was added MeMgCl in THF (3.0 M, 1.13 mL, 3.4 mmol). The suspension was kept at −30 °C (with occasional shaking), as the bright yellow solid was gradually replaced by a white precipitate and yellow solution. After 2 h, 15 mL of precooled (−30 °C) pentane and 2 drops of 1,4-dioxane were added. The suspension was filtered through a bed of Celite (the frit, Celite, and receiving flask had been precooled to −30 °C), the filtrate concentrated until precipitation was observed (~20 mL), and the mixture stored at −30 °C overnight. The fine yellow powder was filtered (precooled frit), washed with cold pentane, and dried in vacuo briefly (10 min). The sample was cooled to −30 °C and placed in vacuo again for 10 min. [t-BuNSN]ZrMe$_2$ was obtained as a fine yellow powder (0.37 g). A second crop (0.18 g) was obtained by concentration of the filtrate to ~10 mL and cooling to −30 °C overnight: total yield 0.55 g (70%); ^{1}H NMR (toluene-d_8, 0 °C) δ 7.25 (dd, 2), 6.95 (td, 2), 6.86 (dd, 2), 6.58 (td, 2), 1.29 (s, 6, CC*H*$_3$(CD_3)$_2$), 1.02 (s, 6, Zr(C*H*$_3$)$_2$); ^{13}C NMR (toluene-d_8, −25 °C) δ 153.4 (br), 134.2 (br), 130.4, 123.4, 122.10 (br), 57.4, 45.9 (Zr-*C*H$_3$), 44.5 (Zr-*C*H$_3$), 30.4, 29.8 (m, $CCH_3(CD_3)_2$).

[i-PrNSN]Zr(NMe$_2$)$_2$. To a solution of $Zr(NMe_2)_4$ (1.08 g, 4.04 mmol) in 5 mL of pentane was added H_2[i-PrNSN] (1.28 g, 4.26 mmol) in 3 mL of pentane. The reaction was complete (by ^{1}H NMR) after 4 h at room temperature. The solvents were removed in vacuo to leave [i-PrNSN]Zr(NMe$_2$)$_2$ as a thick yellow oil: yield 1.98 g (100%). The complex was pure (>95%) by ^{1}H and ^{13}C NMR and was used directly in further reactions. Analytically pure [i-PrNSN]Zr(NMe$_2$)$_2$ could be obtained occasionally in low yield by cooling a saturated pentane solution of the complex to give a yellow solid: ^{1}H NMR (C_6D_6) δ 7.30 (dd, 2), 7.02 (td, 4), 6.65 (dd, 2), 6.49 (td, 2), 3.91 (sept, 2), 2.88 (s, 6, N(C*H*$_3$)$_2$), 2.79 (s, 6, N(C*H*$_3$)$_2$), 1.32 (d, 3, NCH(C*H*$_3$)$_2$), 1.14 (d, 3, NCH(C*H*$_3$)$_2$); ^{13}C NMR (C_6D_6) δ 155.7, 133.8, 130.9, 118.1, 117.6, 116.2, 51.2 (NCH(*C*H$_3$)$_2$), 43.3, 42.1, 23.7 (N*C*H-(CH_3)$_2$), 23.1 (N*C*H(CH_3)$_2$). Anal. Calcd for $C_{22}H_{34}N_4SZr$: C, 55.30; H, 7.17; N, 11.73. Found: C, 55.29; H, 7.30; N, 11.66.

[i-PrNSN]ZrCl$_2$. To a solution of [i-PrNSN]Zr(NMe$_2$)$_2$ (1.88 g, 3.9 mmol) in 20 mL of toluene was added an excess of Me_3-SiCl (1.7 g, 16 mmol). The solution turned yellow, and a yellow precipitate formed within 15 min. After 5 h, 20 mL of pentane was added and the suspension was cooled to −30 °C. After 2 h the fine yellow solid was collected by filtration, washed twice with 40 mL of pentane, and dried in vacuo to give 1.62 g (90%) of analytically pure [i-PrNSN]$ZrCl_2$: ^{1}H NMR (C_6D_6, 500 MHz) δ 7.23 (dd, 2), 6.83 (td, 2), 6.45 (m, 4), 4.63 (sept, 2), 1.29 (s, br, 12, NCH(C*H*$_3$)$_2$); ^{13}C NMR (C_6D_6, 125.8 MHz) δ 155.1, 134.0, 130.5, 121.7, 116.3, 48.9 (NCH(*C*H$_3$)$_2$), 22.3 (N*C*H(CH$_3$)$_2$), 21.2 (N*C*H(CH$_3$)$_2$). Anal. Calcd for $C_{18}H_{22}Cl_2N_2SZr$: C, 46.94; H, 4.81; N, 6.08. Found: C, 46.93; H, 4.78; N, 6.04.

[i-PrNSN]ZrMe$_2$. To a precooled (−30 °C) suspension of [i-PrNSN]$ZrCl_2$ (0.98 g, 2.12 mmol) in 25 mL of diethyl ether was added MeMgCl in THF (3.0 M, 1.4 mL, 4.2 mmol). The suspension was kept at −30 °C (with occasional shaking), as the bright yellow solid was replaced by a white precipitate and pale yellow solution. After 1 h the suspension was filtered through a bed of Celite and the filtrate concentrated to ~3 mL and stored at −30 °C overnight. The light yellow crystals were filtered and washed with 1 mL of cold diethyl ether and then 1 mL of cold pentane. The residual solvent was removed by dissolving the sample in cold (−30 °C) toluene (3 mL) and removing the solvent in vacuo; three repetitions removed >95% of the THF and diethyl ether (by ^{1}H NMR). This procedure also led to a slight darkening of the solution (to yellow-brown), although no change in purity (>98%) was

observed according to NMR (^{1}H, ^{13}C): yield 630 mg of tan powder (71%); ^{1}H NMR (C_6D_6) δ 7.27 (dd, 2), 7.02 (td, 2), 6.65 (dd, 2), 6.48 (td, 2), 4.61 (sept, 2), 1.69 (br s, 6, NCH(CH_3)$_2$), 1.36 (br s, 6, NCH(CH_3)$_2$), 0.61 (br s, 3, Zr−CH_3), 0.26 (br s, 3, Zr−CH_3); ^{13}C NMR (C_6D_6) δ 153.3, 133.4, 130.8, 118.8, 116.9, 114.2, 47.5 (NCH(CH_3)$_2$), 39.5 (br, Zr−CH_3), 22.4 (NCH(CH_3)$_2$), 21.5 (NCH(CH_3)$_2$).

[i-PrNSN]Zr(CH$_2$CHMe$_2$)$_2$. To a precooled (−30 °C) suspension of [i-PrNSN]$ZrCl_2$ (0.50 g, 1.1 mmol) in 25 mL of diethyl ether was added i-BuMgCl (2.0 M, 1.1 mL, 2.2 mmol). The suspension was kept at −30 °C for 1.5 h (with occasional shaking). The suspension was filtered through a bed of Celite. The filtrate was concentrated to ∼2 mL, 2 mL of pentane was added, and the solution was stored at −30 °C overnight. The light yellow crystals were filtered off and washed with 1 mL of cold diethyl ether and then 1 mL of cold pentane. Residual diethyl ether and pentane were removed by dissolving the sample in cold (−30 °C) toluene (3 mL) and removing the solvent in vacuo several times. This procedure also led to a slight darkening of the solution (to orange-yellow), although no change in purity (>98%) was observed by NMR (^{1}H, ^{13}C): yield 410 mg of an orange powder (75%); ^{1}H NMR (C_6D_6, 500 MHz) δ 7.32 (dd, 2), 7.04 (td, 2), 6.76 (dd, 2), 6.54 (td, 2), 4.70 (sept, 2), (s, 6, Zr(CH_3)$_2$), 2.21 (br s, 1, ZrCH_2CHMe$_2$), 2.07 (br s, 1, ZrCH_2CHMe$_2$), 1.78 (br s, 6, NCH(CH_3)$_2$), 1.39 (br s, 6, NCH(CH_3)$_2$), 1.01 (br s, 10, (ZrCH_2CH(CH_3)$_2$), 0.74 (br s, 6, ZrCH$_2$CH(CH_3)$_2$); ^{13}C NMR (C_6D_6, 125.8 MHz) δ 152.4, 133.3, 130.7, 118.8, 116.9, 114.8, 80.1 (Zr−CH_2), 78.1 (Zr−CH_2), 47.8 (NCH(CH_3)$_2$), 28.3, 22.7 (NCH(CH_3)$_2$), 21.7 (NCH(CH_3)$_2$).

"{**[t-BuNSN]ZrMe**}{**B(C$_6$F$_5$)$_4$**}". [t-BuNSN]$ZrMe_2$ (20 mg, 43 μmol) was dissolved in 0.3 mL of precooled chlorobenzene-d_5 and added to a −30 °C solution of [Ph_3C][B(C_6F_5)$_4$] (39 mg, 42 μmol) in 0.3 mL of chlorobenzene-d_5. The initial red-orange solution immediately turned orange-yellow. The sample was kept at −10 °C during transfer to a precooled NMR probe. The ^{1}H NMR spectrum was indicative of clean formation of {[t-BuNSN]ZrMe}{B(C_6F_5)$_4$}: ^{1}H NMR (C_6D_5Cl, −10 °C) δ 7.50−6.98 (m, ∼23), 2.30 (s, 3, Ph_3CCH_3), 1.35 (s, 6, CCH_3(CD_3)$_2$), 1.09 (s, 3, ZrCH_3).

The above reaction was also carried out by utilizing [t-BuNSN]Zr($^{13}CH_3$)$_2$ and [Ph_3C][B(C_6F_5)$_4$]. The resulting ^{13}C NMR spectrum was indicative of clean formation of [t-BuNSN]-Zr($^{13}CH_3$)][B(C_6F_5)$_4$] and $Ph_3C(^{13}CH_3)$: ^{13}C NMR (C_6D_5Cl, −10 °C) 52.8 (br, Zr−$^{13}CH_3$), 31.24 ($Ph_3C-^{13}CH_3$).

Addition of an excess of THF (3 equiv) to a solution of {[t-BuNSN]ZrMe}{B(C_6F_5)$_4$} led to a pale yellow solution. The ^{1}H NMR spectrum was indicative of clean formation of unsymmetric {[t-BuNSN]ZrMe(THF)$_x$}{B(C_6F_5)$_4$}: ^{1}H NMR (C_6D_5Cl, 23 °C) δ 7.60−6.80 (m, ∼23), 3.90 (br s, ∼12, THF), 2.29 (s, 3, Ph_3CCH_3), 1.74 (br s, ∼12, THF), 1.58 (s, 3, CCH_3(CD_3)$_2$), 1.34 (s, 3, CCH_3(CD_3)$_2$), 0.90 (s, 3, ZrCH_3).

Attempted Polymerization of 1-Hexene. [t-BuNSN]-$ZrMe_2$ (21 mg, 46 μmol) was dissolved in 0.3 mL of precooled (−30 °C) chlorobenzene-d_5 and added to a −30 °C solution of [Ph_3C][B(C_6F_5)$_4$] (38 mg, 41 μmol) in 0.3 mL of chlorobenzene-d_5. After 5 min, 10 equiv of 1-hexene (60 μL) was added and the sample stored at −10 °C. After 3 h, the ^{1}H NMR spectrum indicated all 1-hexene was converted to poly(1-hexene). Under similar conditions but with 50−100 equiv of 1-hexene added, only a small portion (10−20 equiv) was polymerized in 3 h.

The reaction was also conducted on a batch scale. [t-BuNSN]-$ZrMe_2$ (22 mg, 48 μmol) was dissolved in 5 mL of precooled (−30 °C) chlorobenzene and added to a −30 °C solution of [Ph_3C][B(C_6F_5)$_4$] (38 mg, 41 μmol) in 5 mL of chlorobenzene. After 5 min, 300 equiv (1.0 g, 1.5 mL) of 1-hexene was added and the reaction mixture was stirred at −10 °C for 3 h. The reaction was quenched by adding 3 mL of 1.0 M HCl in diethyl ether, and the solvents were removed in vacuo to leave 200 mg (20%) of a white sticky residue whose NMR is consistent with poly(1-hexene). Similar yields are obtained if 100 or 500 equiv of 1-hexene is used.

Reaction of [i-PrNSN]ZrMe$_2$ with [PhNMe$_2$][B(C$_6$F$_5$)$_4$]. [i-PrNSN]$ZrMe_2$ (25 mg, 59 μmol) was dissolved in 0.6 mL of bromobenzene-d_5, the solution was cooled to −30 °CC, and slightly less than 1 equiv of powdered [$PhNMe_2$][B(C_6F_5)$_4$] (43 mg, 54 μmol) was added. The reaction mixture was warmed to −10 °C and stirred for 45 min as the color slowly changed to orange-red. The ^{1}H NMR of the sample after ∼50 min was indicative of two main species, **A** (75%) and **B** (25%). ^{1}H NMR (23 °C, C_6D_5Br): δ 7.5−6.5 (m, ∼18, **A** and **B**), 4.16 (sept, ∼1.5, **A**), 4.05 (sept, ∼0.5, **B**), 3.19 (br s, ∼4, **A**/**B**), 3.0 (br s, ∼1, **A**/**B**), 2.92 (s, 3, **A**/**B**), 1.71 (d, ∼6, **A**), 1.46 (d, ∼3, **B**), 1.36 (d, ∼3, **B**), 1.11 (d, ∼6, **A**), 1.04 (s, ∼3, **A**). A mixture of species **A** (50%) and **B** (50%) is also observed if the reaction mixture is warmed to room temperature for 10 min instead of −10 °C for 45 min. The assignment of resonances for **A** and **B** is supported by the observation that, at room temperature, the resonances assigned to **A** decrease in intensity as those of **B** increase until significant decomposition occurs within 90 min at room temperature. Conversion of **A** to **B** is facilitated by heating the sample. Attempts to control the reaction conditions to obtain a clean ^{1}H NMR spectrum of **A** or **B** were unsuccessful.

Acknowledgment. R.R.S. thanks the Department of Energy (Contract No. DE-FG02-86ER13564) and Exxon for supporting this research and the National Science Foundation for funds to help purchase a departmental SMART/CCD diffractometer. R.S. thanks the Alexander von Humboldt Foundation for a Feodor-Lynen-Fellowship. D.D.G. thanks R. Baumann for useful discussions.

Supporting Information Available: Fully labeled ORTEP drawings and tables of atomic coordinates, bond lengths and angles, and anisotropic displacement parameters for [t-BuNSN]ZrCl(NMe$_2$) and [i-PrNSN]$ZrMe_2$. This material is available free of charge via the Internet at http://pubs.acs.org.

OM980934K